Small molecule-mediated inhibition of myofibroblast transdifferentiation for the treatment of fibrosis

Michael J. Bollong[a], Baiyuan Yang[b], Naja Vergani[b], Brittney A. Beyer[b], Emily N. Chin[b], Claudio Zambaldo[a], Danling Wang[b], Arnab K. Chatterjee[b], Luke L. Lairson[a,b,1], and Peter G. Schultz[a,b,1]

[a]Department of Chemistry, The Scripps Research Institute, La Jolla, CA 92037; and [b]California Institute for Biomedical Research, La Jolla, CA 92037

Contributed by Peter G. Schultz, March 23, 2017 (sent for review February 17, 2017; reviewed by Nathanael S. Gray and Laura L. Kiessling)

Fibrosis, a disease in which excessive amounts of connective tissue accumulate in response to physical damage and/or inflammatory insult, affects nearly every tissue in the body and can progress to a state of organ malfunction and death. A hallmark of fibrotic disease is the excessive accumulation of extracellular matrix-secreting activated myofibroblasts (MFBs) in place of functional parenchymal cells. As such, the identification of agents that selectively inhibit the transdifferentiation process leading to the formation of MFBs represents an attractive approach for the treatment of diverse fibrosis-related diseases. Herein we report the development of a high throughput image-based screen using primary hepatic stellate cells that identified the antifungal drug itraconazole (ITA) as an inhibitor of MFB cell fate in resident fibroblasts derived from multiple murine and human tissues (i.e., lung, liver, heart, and skin). Chemical optimization of ITA led to a molecule (CBR-096-4) devoid of antifungal and human cytochrome P450 inhibitory activity with excellent pharmacokinetics, safety, and efficacy in rodent models of lung, liver, and skin fibrosis. These findings may serve to provide a strategy for the safe and effective treatment of a broad range of fibrosis-related diseases.

fibrosis | itraconazole | myofibroblast | transdifferentiation | drug discovery

Fibrosis, generally defined as the production of excessive amounts of extracellular matrix (ECM) components, develops as a consequence of diverse underlying disease (1). Despite the diversity of underlying etiologies that can lead to fibrosis in a given tissue, common biochemical and cellular mechanisms occur in all instances studied to date. An initiating event activates resident fibroblasts (in some cases recruited bone-marrow–derived circulating fibrocytes or epithelial cells that have undergone an epithelial-to-mesenchymal transition), which transdifferentiate into α-smooth muscle actin (αSMA) expressing myofibroblasts (MFBs) that secrete the ECM components required for wound repair (2). For example, in the case of liver fibrosis, a resident quiescent pericyte population, termed hepatic stellate cells (HSCs), transdifferentiates into type I collagen-producing αSMA-expressing fibrogenic HSCs (3). Transforming growth factor-β1 (TGF-β1) mediated SMAD2/3 signaling commonly drives the transdifferentiation of resident fibroblasts or HSCs to MFBs and stimulates production of ECM components in the latter populations (2, 3). These underlying events result in scar formation, which interferes with normal organ function and can lead to a variety of fibrotic diseases, including idiopathic pulmonary fibrosis (IPF), liver fibrosis associated with the later stages of alcoholic and nonalcoholic liver cirrhosis, kidney fibrosis, cardiac fibrosis, scleroderma, and keloid formation resulting from abnormal wound healing (1). Additionally, fibrosis is a key pathological feature associated with chronic autoimmune and infectious diseases (1). As such, fibrosis represents a critically important health problem—nearly half of all natural deaths in the Western world are attributed to chronic fibroproliferative diseases. However, at present there are only two recently approved drugs specifically indicated for the treatment of fibrotic disease. Clearly, the identification of novel antifibrotic drugs represents a major unmet medical need that would have a significant beneficial impact on patients in multiple disease populations.

An attractive approach to discover new agents and biological mechanisms that target diverse fibrotic diseases is to directly target the transdifferentiation pathway responsible for interconversion of quiescent fibroblasts to activated, profibrotic MFBs. Drugs capable of blocking the conversion of fibroblasts to activated MFBs could act to prevent the progression of disease or even reverse fibrosis in organs capable of repair (e.g., liver fibrosis). Moreover, agents capable of inhibiting the formation of MFBs in the presence of TGF-β1 without directly inhibiting TGF-β1 signaling itself, may have an advantage over direct suppression of TGF-β1, which has the potential to exacerbate immune responses. Cell-based phenotypic screens have proven an effective strategy to identify molecules that affect cell fate by previously unknown mechanisms (4, 5). Herein we undertook an image-based screen of MFB transdifferentiation that led to the discovery of an antifibrotic agent with excellent preclinical in vivo activity and that acts by a unique mechanism of action.

Results

An Image-Based Screen Identifies Itraconazole as an Inhibitor of MFB Differentiation. To identify small drug-like molecules that inhibit the formation of MFBs, we developed a miniaturized high-content imaging assay using primary HSCs, which have been demonstrated to contribute to over 90% of the fibrosis-associated MFBs in livers of carbon tetrachloride (CCl_4)-injured mice and remain sensitive to TGF-β–induced MFB formation in vitro (3, 6). A hallmark of the MFB cell state is the acquisition of an elaborated αSMA network accompanied by a marked increase in cell size (2, 7). First passage HSCs were treated with TGF-β1 under conditions where

Significance

The treatment of fibrosis remains a critically important unmet medical need, as nearly 45% of all natural deaths in the Western world are attributed to chronic fibroproliferative disease complications. Fibrosis is characterized by the excessive deposition of extracellular matrix proteins by resident fibroblast-derived myofibroblasts. From an imaging-based screen, we identified the antifungal drug itraconazole as an inhibitor of myofibroblast transdifferentiation from multiple resident fibroblast populations. A derivative of this drug was found to inhibit fibrotic disease progression in mouse models of lung, liver, and skin fibrosis, demonstrating that inhibiting differentiation to the myofibroblast cell state is a practical strategy to treat a wide range of fibrosis-related diseases.

Author contributions: M.J.B., B.Y., D.W., A.K.C., L.L.L., and P.G.S. designed research; M.J.B., B.Y., N.V., B.A.B., E.N.C., C.Z., and D.W. performed research; M.J.B., B.Y., N.V., B.A.B., E.N.C., C.Z., D.W., A.K.C., L.L.L., and P.G.S. analyzed data; and M.J.B., L.L.L., and P.G.S. wrote the paper.

Reviewers: N.S.G., Harvard Medical School; and L.L.K., University of Wisconsin–Madison.

The authors declare no conflict of interest.

[1]To whom correspondence may be addressed. Email: schultz@scripps.edu or llairson@scripps.edu.

This article contains supporting information online at www.pnas.org/lookup/suppl/doi:10.1073/pnas.1702750114/-/DCSupplemental.

CELL BIOLOGY

quiescent HSCs and MFBs could be distinguished using a high-content imaging algorithm that measured both cellular size and staining intensity for αSMA (*SI Appendix*, Fig. S1 *A* and *B*). We adapted this assay to a high-throughput format and subsequently screened a collection of ∼80,000 structurally diverse small molecules, including known biologically active compounds. Among those compounds deemed "hits" were both novel chemical scaffolds as well as known modulators of HSC fate, including ligands for peroxisome proliferator-activated receptor gamma and inhibitors for the platelet-derived growth factor receptor (*SI Appendix*, Fig. S1*C*). Among the most promising lead compounds for which antifibrotic activity had not been previously reported was the triazole antifungal itraconazole (ITA), a well-tolerated drug that has been used clinically for over 25 y. Indeed, ITA was found to dose dependently decrease MFB formation with a half-maximal inhibitory concentration (IC_{50}) of ∼300 nM, efficacy comparable to that of the TGF-β1 signaling inhibitor SB-431542 (a selective ALK5 inhibitor), which served as our positive control (Fig. 1 *A* and *B*). Interestingly, other classes of antifungal agents were not active in this assay, suggesting that ITA's ability to inhibit MFB formation may be due to a distinct activity of this drug. This observation, the large amount of clinical data available for ITA, and a clinical observation in the literature that ITA treatment is beneficial to patients with keloids with accompanying fungal infections led us to further investigate its in vitro and in vivo activity (8).

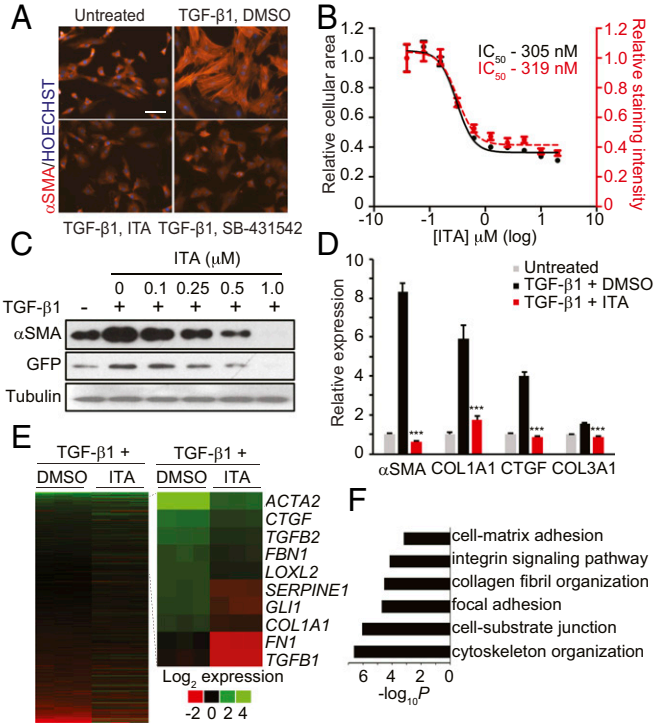

Fig. 1. ITA inhibits MFB transdifferentiation. (*A*) Images of rat HSCs treated with ITA (0.5 μM) or SB-431542 (10 μM) in MFB formation conditions immunostained for αSMA (Scale bar, 100 μm). (*B*) Image analysis quantification of rat HSCs treated with ITA in MFB formation conditions ($n = 9$, mean and SEM). (*C*) Western blot analyses of αSMA and GFP from COL1–GFP HSCs subjected to MFB conditions and treated with ITA. (*D*) qRT-PCR analyses of MFB identity genes from human lung fibroblasts (HLFs) treated for 72 h (ITA, 0.3 μM; $n = 3$, mean and SD; $^{***}P < 0.0005$, *t* test). (*E*) Heatmap displaying the $\log_2$ fold change from untreated controls of all active transcripts (*Left*) or core MFB genes (*Right*) as measured by RNA-seq from HLFs treated with TGF-β1+DMSO or ITA (300 nM) for 72 h. (*F*) Enrichment *P* values from DAVID analyses for selected GO categories of genes up-regulated by TGF-β1 but suppressed by ITA treatment.

In Vitro Biological Activity of ITA. As expected, ITA-induced inhibition of MFB formation leads to down-regulation of the mRNA transcript and/or protein levels of key genes of MFB identity, including αSMA, collagen type 1 alpha 1 (COL1A1), fibronectin, and TGF-β1, in primary rat HSCs following exposure to TGF-β1–containing transdifferentiation medium (Fig. 1*C* and *SI Appendix*, Fig. S2 *A–C*). ITA was not found to inhibit TGF-β1–induced SMAD2 or SMAD3 phosphorylation or exhibit any inhibitory activity in a SMAD binding element-based reporter assay (4xSBE-LUC), indicating that the compound does not act by directly inhibiting TGF-β signaling, as is the case with the SB-431542 (*SI Appendix*, Fig. S2 *D* and *E*). Whereas ITA was found to display antiproliferative activity in HSCs, as evidenced by a dose-dependent decreases in cyclin A (*SI Appendix*, Fig. S2*F*), the compound was not found to induce apoptosis at concentrations below 20 μM (*SI Appendix*, Fig. S2*G*) or induce general cytotoxicity at the concentrations reported for in vitro experiments.

Next we evaluated the activity of ITA in fibroblasts derived from other organs in which the majority of disease-associated MFBs are derived from transdifferentiation of resident fibroblasts. We found that ITA concentrations of less than 1 μM were capable of antagonizing TGF-β1–stimulated changes in cellular morphology or αSMA expression levels in human or rat lung fibroblasts, rat cardiac fibroblasts, rat dermal fibroblasts, and human or rat hepatic stellate cells (*SI Appendix*, Fig. S3 *A* and *B*). Further characterization of human lung fibroblasts revealed that ITA could broadly inhibit the expression of MFB-associated genes, as measured by both Western blotting and qRT-PCR analysis (Fig. 1*D* and *SI Appendix*, Fig. S3 *C* and *D*). To evaluate the transcriptome-wide changes induced by ITA treatment, we performed RNA-seq expression profiling on human lung fibroblasts exposed to MFB formation conditions. ITA was found to significantly suppress a substantial fraction of transcripts up-regulated (371 of 858) or down-regulated (720 of 1908) by TGF-β1 treatment (*SI Appendix*, Fig. S4 *A–C*). Consistent with our qRT-PCR results, ITA was found to suppress the expression of core genes of MFB identity as well as inhibit the expression of gene classes involved with MFB function (Fig. 1 *D* and *E*) (9). Additionally, gene set enrichment analysis revealed that ITA significantly affected the expression of TGF-β1 target and hallmark EMT gene sets, a result comparable to gene set enrichment analyses results obtained comparing untreated to TGF-β1–treated samples (*SI Appendix*, Fig. S4 *D–G*) (10). Together, these results demonstrate that ITA functionally antagonizes a core transcriptional program involved in the establishment of MFB cell fate but does not globally suppress all transcripts modulated by TGF-β1 treatment, further confirming that ITA does not act by direct TGF-β–signaling inhibition.

Recently, it has been shown that HSC-derived CCl_4-induced MFBs are capable of dedifferentiating to a quiescent phenotype following withdrawal of CCl_4 administration, indicating the MFB cellular state does not represent a terminal differentiation endpoint but rather a transient and malleable cellular identity (6, 11). To determine whether ITA could induce the reversion of MFBs back to a quiescent state in vitro, primary rat HSCs were transdifferentiated for 48 h and then treated with ITA in the presence of TGF-β1–containing transdifferentiation media for 96 h. Cell state was then assessed by evaluating gross cellular morphology and the transcript levels of MFB identity genes. Interestingly, compound treatment was found to decrease transcript levels of COL1A1 and αSMA as well as decrease cell size and the organization of the intracellular αSMA network (*SI Appendix*, Fig. S5 *A–D*). Further, it was found that if ITA was removed from the transdifferentiation culture media following 96 h of treatment of existing MFBs, the cells rebounded to a MFB state and reexpressed comparable levels of αSMA in the presence of TGF-β1 (*SI Appendix*, Fig. S5*C*). These results indicate that the cellular effects induced by ITA are a sufficient stimulus to override the MFB

differentiation program and revert the cell to a less activated state. Additionally, these results also suggest that these effects are not the result of a general toxicity-based mechanism, as changes in αSMA content are readily reversed by compound washout. Consistent with a lack of reported reversion capacity for other MFB populations, ITA was not found to induce the reversion of MFBs derived from human lung fibroblasts (*SI Appendix*, Fig. S5*E*).

Mechanistic Studies of ITA's Anti-MFB Formation Activity. Although initially developed as an antifungal antibiotic, ITA has been shown to inhibit Hedgehog (Hh) pathway and vascular endothelial growth factor (VEGF) signaling (12, 13). Both pathways are known to influence the MFB cell state and have been proposed as potential targets for the development of antifibrotic therapeutics (14–17). Consistent with these observations, we found that the mRNA transcript levels of multiple VEGF and Hh signaling components are elevated in HSCs following MFB differentiation (*SI Appendix*, Fig. S6*A*). Also consistent with previous reports, ITA was found to inhibit both SAG- and N-terminal Sonic Hedgehog (SHH-N)-induced patched (PTCH1) and GLI family zinc finger 1 (GLI1) gene expression in rat HSCs as well as dose-dependently inhibit SAG-induced GLI-dependent transcription (*SI Appendix*, Fig. S6 *B–D* and Fig. 2*D*). Inhibition of the VEGF pathway by ITA has been attributed to inhibition of VEGF receptor glycosylation and trafficking to the cell membrane (12). In rat HSCs, ITA was found to cause a decrease in the observed molecular weight of VEGFR2 by Western blot analysis, indicating a loss of receptor glycosylation (*SI Appendix*, Fig. S6*F*). Additionally, ITA inhibited the VEGF-dependent proliferation of human HSCs when supplemented with VEGF in serum-free medium (*SI Appendix*, Fig. S6*G*). We therefore evaluated the role of these mechanisms in the observed antifibrotic activity of ITA using pharmacological inhibitors. Whereas inhibition of either Hh signaling (cyclopamine, 5 μM) or VEGF signaling (KRN-633, 0.5 μM) pathways at maximally efficacious but nontoxic doses individually resulted in partial inhibition of MFB activation in rat HSCs, complete recapitulation of the antifibrotic activity of ITA was only achieved using a combination of the individual inhibitors (*SI Appendix*, Fig. S6*H*). Together, these results demonstrate that ITA functionally antagonizes Hh and VEGF signaling pathways in HSCs and are consistent with the hypothesis that ITA's inhibitory effect on MFB transdifferentiation is derived from fortuitous dual inhibition of two known profibrotic signaling pathways (i.e., VEGF and Hh signaling).

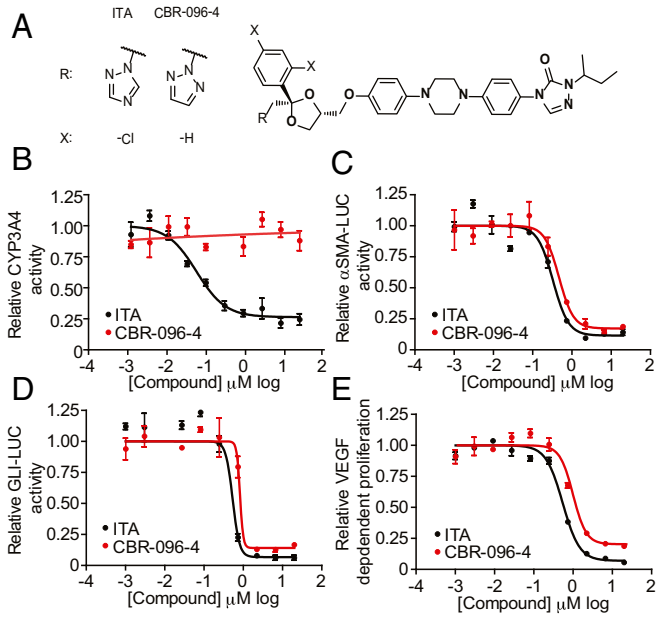

Fig. 2. CBR-096-4, an antifibrotic agent with no CYP3A4 inhibitory activity. (*A*) Structures of ITA and CBR-096-4. (*B*) Results of CYP3A4 in vitro activity (*B*), αSMA-luciferase (*C*), GLI-luciferase (*D*), and VEGF-dependent proliferation (*E*) assays in the presence of indicated doses of ITA and CBR-096-4 ($n = 3$, mean and SEM).

A Preliminary Structure Activity Analysis of ITA Activity. ITA's antifungal activity results from inhibition of the essential yeast P450 enzyme lanosterol 14-α-demethylase (18). Unfortunately, ITA also inhibits human liver P450 enzymes, most notably CYP3A4, which makes it unattractive as an antifibrotic agent due to both potential hepatotoxicity (especially in liver fibrosis) and to potential drug–drug interactions with other agents in an antifibrotic drug regimen. To overcome these limitations, and to determine whether we could dissociate the antifungal activity of ITA from its antifibrotic activity, we carried out a preliminary structure activity relationship (SAR) analysis on ITA. Because ITA inhibits P450 enzymes via coordination of the basic N4 nitrogen of its triazole moiety to heme iron (19), we reasoned that substitution of this nitrogen or modulation of its pK_a would decrease binding affinity to CYP3A4. Several analogs were synthesized in which the 1,2,4-triazole moiety was substituted with electron withdrawing groups (e.g., −Br, $-CF_3$ at position 3) or replaced with isosteric ring systems (e.g., pyrazole, 1,2,3-triazole, pyridine, pyridazine). Compounds were identified that have little to no CYP3A4 inhibitory activity and as a consequence lack antifungal activity, but were active in the MFB formation assay as determined by Western blot analysis of transdifferentiated human lung fibroblasts. These results confirmed that the antifibrotic activity of ITA is not derived from on-target inhibition of a CYP enzyme. Unfortunately, most compounds were significantly less potent with respect to ITA itself, and therefore several of these CYP inactive analogs were subjected to subsequent rounds of SAR to optimize their in vitro potency and pharmacological properties. We found that the diphenylpiperazine, triazolinone, and sec-butyl side chain regions were essential to ITA's activity in MFB formation assays and that only minor improvements in potency were achieved by modifying these regions. In contrast, altering the substitution pattern and identity of withdrawing groups on ITA's dichlorophenyl moiety afforded the greatest improvements in potency in the context of analogs containing isosteric replacements of the 1,2,4-triazole. From a medicinal chemistry campaign involving over 300 ITA analogs, we ultimately identified a 1,2,3-triazole and unsubstituted phenyl-containing analog, termed CBR-096-4, which retains the anti-MFB efficacy of ITA and displays no CYP3A4 inhibitory or antifungal activity (Fig. 2 *A* and *B* and *SI Appendix*, Fig. S7*A*). Like ITA, CBR-096-4 inhibited the formation of MFBs from multiple tissue types as determined by Western blotting and immunofluorescent staining (*SI Appendix*, Fig. S7 *B* and *C*). We also found that CBR-096-4 inhibits Hedgehog reporter activity (GLI-LUC), VEGF-dependent growth, and αSMA-LUC reporter activity with similar potency to ITA, suggesting that CBR-096-4 functions by the same mechanism of action as ITA (Fig. 2 *C–E*). This analog was also found to be inactive against multiple mouse and human CYP enzymes and was also inactive in CYP induction and PXR activation assays (*SI Appendix*, Fig. S7 *D* and *E*). Furthermore, CBR-096-4 retained similar pharmacokinetic properties to ITA in rodents, which likely makes it amenable to once-a-day oral delivery (*SI Appendix*, Fig. S7 *F* and *G*).

CBR-096-4 Decreases Disease Burden in Multiple Rodent Models of Fibrotic Disease. Encouraged by the cross-species in vitro antifibrotic activity of CBR-096-4 in assays based on fibroblasts derived from multiple organs, we examined its in vivo efficacy in multiple rodent models of fibrotic disease. We first evaluated the ability of CBR-096-4 to inhibit fibrotic disease progression in the

CELL BIOLOGY

bleomycin-induced lung fibrosis model. Despite some inherent limitations in modeling the human disease, both clinically approved antifibrotic drugs have shown efficacy in the bleomycin mouse model (14, 20, 21). This model typically involves either repetitive s.c. injection of bleomycin or a one-time intratracheal injection of the drug (22). The former method has been criticized for its inability to separate antiinflammatory from antifibrotic effects, whereas the latter method frequently suffers from high interanimal variability in inducing fibrotic disease (21, 23). To separate the inflammatory phase of this model from the subsequent fibrotic stages, we chose to administer bleomycin (25 mg/kg) via a subdermally implanted osmotic pump for 7 d, after which time the pump was surgically removed, and mice were left untreated for 7 d for inflammation to subside and fibrotic progression to begin (*SI Appendix*, Fig. S8*A*). Based on the established pharmacokinetic (PK) of CBR-096-4 in mice [6.7 h half-life; 2,013 ng/mL C_{max}; 27,171 h·ng/mL area under the curve (AUC)], mice were then dosed once daily [1–25 mg/kg, orally dosed (P.O.)] for 2 wk with no significant effect on body weight (*SI Appendix*, Fig. S8*B*). As positive controls, we used AM152, an LPA1 receptor antagonist, which acts by inhibiting fibroblast trafficking and vascular leakage (24), and pirfenidone, an FDA-approved antifibrotic drug, which has been reported to act by a number of antifibrotic mechanisms (20). CBR-096-4 (10 mg/kg) had a similar level of antifibrotic activity, as determined by histological Ashcroft scoring and automated image analysis for collagen staining (described in *Methods*), compared with the maximally efficacious doses of AM152 (once daily P.O. at 30 mg/kg) or pirfenidone (twice daily P.O. at 400 mg/kg) (Fig. 3 *A–C* and *SI Appendix*, Fig. S8 *C–E*). Furthermore, we observed a significant decrease in total αSMA positive area in CBR-096-4–treated mice, as determined by immunohistochemical staining (Fig. 3 *D* and *E*), a result consistent with the idea that CBR-096-4 functions by directly inhibiting the formation of MFBs under profibrotic conditions.

We further evaluated the ability of CBR-096-4 to inhibit fibrotic disease progression in the commonly used CCl_4-induced liver fibrosis model (25). In this model the hepatotoxic agent CCl_4 (0.4 mL/kg) is administered twice weekly for 5 wk to induce fibrosis and drug treatment is initiated during weeks 3 and 4. Dosing mice with CBR-096-4 (once daily P.O. at 10 mg/kg) resulted in significant decreases in percent Sirius Red (a stain for type I and III collagen) positive area with respect to vehicle controls (Fig. 3 *F* and *G*), indicating that total collagen deposition in the liver was decreased with compound treatment. This activity was comparable to that of a maximally efficacious dose (once daily P.O. at 30 mg/kg) of AM152. CBR-096-4 was further evaluated using a bleomycin-induced skin fibrosis model (26). Here, a bleomycin solution (20 μg) was s.c. injected once daily into a conserved dorsal injection site for

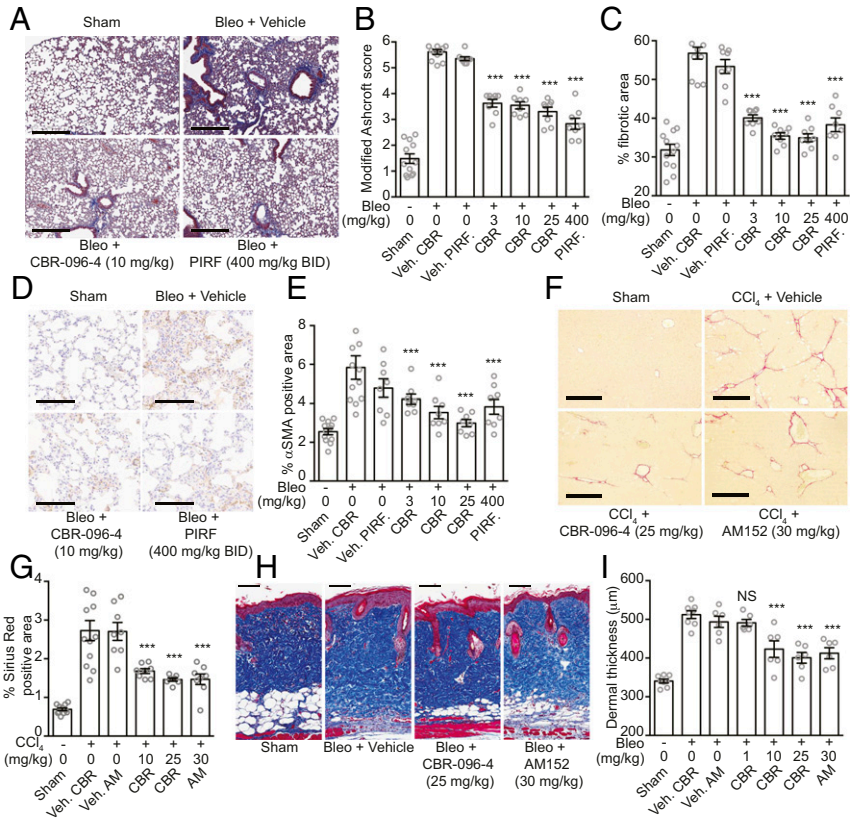

Fig. 3. CBR-096-4 decreases disease severity in rodent models of fibrotic disease. (*A*) Representative Masson's trichrome-stained lung sections from mice subjected to bleomycin treatment. (Scale bars, 300 μm.) Modified Ashcroft scores (*B*) and histological staining quantification of percent fibrotic area (*C*) from the bleomycin-induced lung fibrosis model. (*D*) Representative lung sections immunostained for αSMA from mice subjected to bleomycin treatment. (Scale bars, 100 μm.) (*E*) Quantification of percent αSMA positive area measurements from the bleomycin-induced lung fibrosis model. Images of representative Sirius Red-stained liver sections (*F*) and quantification of total Sirius Red positive area (*G*) for indicated treatment groups from mice subjected to the CCl_4-induced liver fibrosis model. (Scale bars, 400 μm.) Representative images of Masson's trichrome-stained skin sections (*H*) and quantification of dermal thickness (*I*) from mice exposed to the bleomycin-induced skin fibrosis model. (Scale bars, 100 μm.) ($n = 8$ per treatment group; mean and SEM; white circles indicate mean measurements from individual animals; ***$P < 0.0005$, NS, not significant, one-way ANOVA with Dunnett's correction.) (AM, AM152; BID, twice daily; CBR, CBR-096-4; PIRF, pirfenidone; Veh. AM, AM152 vehicle; Veh. CBR, CBR-096-4 vehicle; and Veh. PIRF, pirfenidone vehicle.)

4 wk with compounds dosed daily during weeks 3 and 4. Disease severity was determined at the end of the study by measuring dermal thickness at sites adjacent to the injection area. CBR-096-4 and AM152 (10 and 30 mg/kg once daily P.O., respectively) both significantly decreased dermal thickness (Fig. 3 *H* and *I*), indicating a decrease in collagen deposition and resident dermal fibroblast proliferation. Consistent with our in vitro results, together these data provide in vivo evidence that CBR-096-4 can function broadly as an antifibrotic agent.

Fibroblast activation and migration is a critical step for ensuring proper wound healing (7). To confirm that CBR-096-4 did not inhibit any necessary processes associated with normal wound healing, we used an excisional wound closure model in which C57BL/6J mice were cutaneously wounded using a biopsy punch and the relative diameter of the wound was measured daily until wound closure (14 d). Neither ITA nor CBR-096-4 (25 mg/kg each) inhibited the degree or rate of cutaneous wound healing (*SI Appendix*, Fig. S9 *A* and *B*). Although MFB activation has been established as a necessary process during normal wound healing, the fact that neither CBR-096-4 nor ITA inhibited wound closure may indicate differences in fibrotic MFB activation and the MFB activation associated with normal wound healing as has been reported in the literature (27). Additionally, neither ITA nor CBR-096-4 were found to significantly reduce body weight over this treatment period (*SI Appendix*, Fig. S9*C*). Finally, to confirm that CBR-096-4 did not induce any adverse effects on gross physiological function, we performed a 7-d rat toxicity study in which CBR-096-4 was administered daily at 100 mg/kg P.O., a dose projected to be 25 times that of a maximally efficacious dose in rats based on observed AUC values. CBR-096-4 was found to have no obvious effects on standard measures of toxicity, including body weight, blood chemistry, hematological composition, and organ weight.

Discussion

Using a phenotypic high-throughput screen involving primary rat HSCs, we have shown that ITA, a widely used approved drug, effectively inhibits the transdifferentiation process involved in the formation of activated MFBs, the causative cell of fibrotic disease pathology. This activity is maintained across multiple rodent and human organ types, suggesting that ITA's mechanism of action represents a conserved and generalizable method for overriding the differentiation cues induced by TGF-β1. In contrast to other investigational therapies aimed at dampening TGF-β signaling (e.g., fresolimumab, STX-100, and LY2382770), our results indicate that ITA does not directly antagonize TGF-β signaling at the ALK5 receptor/SMAD level (28). Whereas inhibiting TGF-β signaling is efficacious at halting disease progression in a number of fibrotic disease models and is currently under clinical evaluation as an antifibrotic therapy, TGF-β also plays a key antiinflammatory role in tuning immunological responsiveness (28). Indeed, positive TGF-β signaling is suppressive of the differentiation and proliferation of T_H1 and T_H2 T cells and is necessary for the instruction of $FOXP3^+$ T_{reg} cells required for peripheral tolerance (29). Given the clear autoimmune component of certain fibrotic diseases (e.g., scleroderma), we speculate that targeting the downstream transcriptional effects in the pathological cell of interest (i.e., the MFB) has the potential to overcome immunological concerns associated with long-term TGF-β signaling inhibition that would be required for antifibrotic therapy.

In agreement with our observation that Hh and VEGF signaling components are up-regulated upon MFB differentiation, the increased expression of Hh and VEGF-related factors has been demonstrated as a salient feature of fibroblasts and tissue derived from patients of multiple fibrotic disease backgrounds (30–32). Additionally, the exogenous expression of either Hh or VEGF has been shown to additively contribute to TGF-β–driven fibrotic disease progression in animal models (33–35). Our results demonstrate that ITA antagonizes both Hh and VEGF signaling pathways in HSCs and that chemical inhibition of both signaling pathways together is sufficient to recapitulate ITA's inhibitory effect on MFB formation. Given the established fibrosis-promoting effects of these pathways, we speculate that ITA's ability to inhibit both Hh and VEGF simultaneously would likely provide therapeutic benefit over inhibiting either pathway alone. Despite the MFB-promoting effects of Hh and VEGF, some examples from the literature suggest that Hh and VEGF may also aid in repopulating and vascularizing the parenchymal epithelium of a given tissue in later stages of fibrotic disease (17, 33). Clearly, further investigation is necessary to fully understand the pleiotropic effects of inhibiting Hh and VEGF signaling pathways as an antifibrotic strategy.

Evidence from Liu and colleagues (12) and Liu and Beachy and colleagues (13) has suggested that ITA inhibits Hh and VEGF pathways by a mechanism involving obstructed trafficking of cell-surface–bound signaling receptors (i.e., Smoothened to the primary cilium and VEGFR2 to the cell surface). Additionally, others have shown that ITA affects the glycosylation and trafficking of other cell surface molecules including CD14 and Fc receptors; however, the relevant cellular target responsible for ITA's effects on receptor trafficking remains unknown (36, 37). Recently, others have reported that ITA inhibits enterovirus replication by binding to oxysterol binding protein (OSBP) and that ITA modulates mTORC1 activity by inhibiting the mitochondrial protein voltage-dependent anion channel 1 (VDAC1) (38, 39). Further mechanistic deconvolution of ITA should clarify whether additional cell types and/or physiological responses might contribute to the antifibrotic efficacy observed in vivo, an important limitation to the current study.

Although ITA has been clinically used for over 25 y with relative safety as an antifungal agent, ITA carries an FDA black box warning for drug–drug interactions due to its potent inhibitory effect on CYP3A4, which is undesirable in an antifibrotic therapeutic regime that will likely involve multiple drugs. In an attempt to leverage the defined pharmacokinetic properties of ITA but eliminate its CYP-inhibitory activity, we undertook a medicinal chemistry campaign, which ultimately identified CBR-096-4, an analog with no CYP-inhibitory profile but retained inhibitory activity in Hh, VEGF, and MFB formation assays with similar potency to ITA. CBR-096-4 was found to reduce disease severity in multiple rodent models of fibrotic disease with levels of efficacy that are comparable to or better than those of late-stage clinical and recently approved antifibrotic drugs. Additionally, CBR-096-4 was found to inhibit the accumulation of αSMA positive MFBs in response to bleomycin damage, indicating that the primary mode of antifibrotic efficacy is derived from inhibiting the accumulation of disease-associated MFBs in response to fibrotic cues and that inhibiting the differentiation of MFBs is a therapeutically relevant mechanism for inhibiting fibrotic disease progression. Given the enhanced safety properties of CBR-096-4 and its antifibrotic efficacy in multiple organs, we speculate CBR-096-4 may be of general clinical utility in treating a number of fibrotic diseases. Together, our results highlight the utility of using unbiased cell-based screens to identify molecules that affect cell fate by uncharacterized mechanisms and further validate the notion that repurposed drugs can lead to accelerated development timelines and predictable safety outcomes for treating diseases with unmet medical need.

Methods

Fibroblast Cell Sources. Rat hepatic stellate cells and human lung fibroblasts were purchased from ScienCell Research Laboratories. Rat lung, dermal, and cardiac fibroblasts are from Cell Applications, Inc. LX1 and LX2 human hepatic stellate cells were a gift from Scott Friedman, Mount Sinai Hospital,

New York, and COL1-GFP HSCs were a gift of David Brenner, University of California, San Diego.

High-Throughput Screening and High-Content Image Analysis. First-passage rat HSCs were plated at a density of 350 cells per well on poly-D-lysine (PDL, 10 μg/mL)-coated 384-well plates (Greiner) in stellate cell medium (ScienCell). After a 24-h recovery, medium was replaced with basal medium lacking growth factors and serum. After 24-h serum starvation, medium was switched to stellate cell medium with added TGF-β1 (10 ng/mL; Gibco) and compounds (5 μM) were subsequently transferred using a Biomek FX workstation affixed with a pintool head. After 48 h, cells were fixed with a 4% paraformaldehyde solution for 10 min and subsequently blocked for 30 min (5% FBS, 0.3% Triton X-100 in PBS) and then stained overnight at 4 °C with primary antibody against αSMA (1% FBS, 0.1% Triton X-100 in PBS). After washing, cells were stained with secondary antibody (donkey anti-mouse Alexa Fluor 488, Invitrogen; 1:500) and Hoechst dye (2 μg/mL) for 2 h at room temperature in the dark. Cells were then washed three times with PBS and sealed for imaging. High-content imaging was performed with a Cellomics Cell Insight imager (Thermo). Four imaging fields per well captured with a 5× imaging objective allowed for visualization of the entire well. For analysis, relative cell area and relative staining intensity for αSMA were determined using internal algorithms in the Cellomics Scan software package and thresholds fitted using multiple wells of positive (SB-431542, 10 μM) and negative (DMSO, 0.1%) controls present in each screening plate.

Animal Use Statement. All experiments were performed in accordance with methods approved by the Institutional Animal Care and Use Committee at the California Institute of Biomedical Research.

ACKNOWLEDGMENTS. We thank G. Welzel, D. Caballero, and J. Gonzales for technical support. This work was supported by the Skaggs Institute for Chemical Biology.

1. Rockey DC, Bell PD, Hill JA (2015) Fibrosis: A common pathway to organ injury and failure. *N Engl J Med* 372:1138–1149.
2. Wynn TA, Ramalingam TR (2012) Mechanisms of fibrosis: Therapeutic translation for fibrotic disease. *Nat Med* 18:1028–1040.
3. Friedman SL (2008) Hepatic stellate cells: Protean, multifunctional, and enigmatic cells of the liver. *Physiol Rev* 88:125–172.
4. Deshmukh VA, et al. (2013) A regenerative approach to the treatment of multiple sclerosis. *Nature* 502:327–332.
5. Johnson K, et al. (2012) A stem cell-based approach to cartilage repair. *Science* 336: 717–721.
6. Kisseleva T, et al. (2012) Myofibroblasts revert to an inactive phenotype during regression of liver fibrosis. *Proc Natl Acad Sci USA* 109:9448–9453.
7. Hinz B (2007) Formation and function of the myofibroblast during tissue repair. *J Invest Dermatol* 127:526–537.
8. Chui CH (2008) Treatment of keloids with itraconazole. *Plast Reconstr Surg* 122: 681–682.
9. Huang W, Sherman BT, Lempicki RA (2009) Systematic and integrative analysis of large gene lists using DAVID bioinformatics resources. *Nat Protoc* 4:44–57.
10. Subramanian A, et al. (2005) Gene set enrichment analysis: A knowledge-based approach for interpreting genome-wide expression profiles. *Proc Natl Acad Sci USA* 102: 15545–15550.
11. Troeger JS, et al. (2012) Deactivation of hepatic stellate cells during liver fibrosis resolution in mice. *Gastroenterology* 143:1073–1083 e1022.
12. Nacev BA, Grassi P, Dell A, Haslam SM, Liu JO (2011) The antifungal drug itraconazole inhibits vascular endothelial growth factor receptor 2 (VEGFR2) glycosylation, trafficking, and signaling in endothelial cells. *J Biol Chem* 286:44045–44056.
13. Kim J, et al. (2010) Itraconazole, a commonly used antifungal that inhibits Hedgehog pathway activity and cancer growth. *Cancer Cell* 17:388–399.
14. Chaudhary NI, et al. (2007) Inhibition of PDGF, VEGF and FGF signalling attenuates fibrosis. *Eur Respir J* 29:976–985.
15. Horn A, et al. (2012) Inhibition of hedgehog signalling prevents experimental fibrosis and induces regression of established fibrosis. *Ann Rheum Dis* 71:785–789.
16. Park HY, Kim JH, Park CK (2013) VEGF induces TGF-β1 expression and myofibroblast transformation after glaucoma surgery. *Am J Pathol* 182:2147–2154.
17. Michelotti GA, et al. (2013) Smoothened is a master regulator of adult liver repair. *J Clin Invest* 123:2380–2394.
18. Georgopapadakou NH, Walsh TJ (1996) Antifungal agents: Chemotherapeutic targets and immunologic strategies. *Antimicrob Agents Chemother* 40:279–291.
19. Isoherranen N, Kunze KL, Allen KE, Nelson WL, Thummel KE (2004) Role of itraconazole metabolites in CYP3A4 inhibition. *Drug Metab Dispos* 32:1121–1131.
20. Schaefer CJ, Ruhrmund DW, Pan L, Seiwert SD, Kossen K (2011) Antifibrotic activities of pirfenidone in animal models. *Eur Respir Rev* 20:85–97.
21. Degryse AL, Lawson WE (2011) Progress toward improving animal models for idiopathic pulmonary fibrosis. *Am J Med Sci* 341:444–449.
22. Moore BB, Hogaboam CM (2008) Murine models of pulmonary fibrosis. *Am J Physiol Lung Cell Mol Physiol* 294:L152–L160.
23. Chaudhary NI, Schnapp A, Park JE (2006) Pharmacologic differentiation of inflammation and fibrosis in the rat bleomycin model. *Am J Respir Crit Care Med* 173: 769–776.
24. Swaney JS, et al. (2010) A novel, orally active LPA(1) receptor antagonist inhibits lung fibrosis in the mouse bleomycin model. *Br J Pharmacol* 160:1699–1713.
25. Iredale JP (2007) Models of liver fibrosis: Exploring the dynamic nature of inflammation and repair in a solid organ. *J Clin Invest* 117:539–548.
26. Yamamoto T, et al. (1999) Animal model of sclerotic skin. I: Local injections of bleomycin induce sclerotic skin mimicking scleroderma. *J Invest Dermatol* 112:456–462.
27. Rinkevich Y, et al. (2015) Skin fibrosis. Identification and isolation of a dermal lineage with intrinsic fibrogenic potential. *Science* 348:aaa2151.
28. Akhurst RJ, Hata A (2012) Targeting the TGFβ signalling pathway in disease. *Nat Rev Drug Discov* 11:790–811.
29. Rubtsov YP, Rudensky AY (2007) TGFbeta signalling in control of T-cell-mediated self-reactivity. *Nat Rev Immunol* 7:443–453.
30. Kajihara I, et al. (2013) Scleroderma dermal fibroblasts overexpress vascular endothelial growth factor due to autocrine transforming growth factor β signaling. *Mod Rheumatol* 23:516–524.
31. Horn A, et al. (2012) Hedgehog signaling controls fibroblast activation and tissue fibrosis in systemic sclerosis. *Arthritis Rheum* 64:2724–2733.
32. Bolaños AL, et al. (2012) Role of Sonic Hedgehog in idiopathic pulmonary fibrosis. *Am J Physiol Lung Cell Mol Physiol* 303:L978–L990.
33. Farkas L, et al. (2009) VEGF ameliorates pulmonary hypertension through inhibition of endothelial apoptosis in experimental lung fibrosis in rats. *J Clin Invest* 119: 1298–1311.
34. Kugler MC, Joyner AL, Loomis CA, Munger JS (2015) Sonic hedgehog signaling in the lung. From development to disease. *Am J Respir Cell Mol Biol* 52:1–13.
35. Liu L, et al. (2013) Hedgehog signaling in neonatal and adult lung. *Am J Respir Cell Mol Biol* 48:703–710.
36. Frey T, De Maio A (2009) The antifungal agent itraconazole induces the accumulation of high mannose glycoproteins in macrophages. *J Biol Chem* 284:16882–16890.
37. Niño DF, Cauvi DM, De Maio A (2014) Itraconazole, a commonly used antifungal, inhibits Fcγ receptor-mediated phagocytosis: Alteration of Fcγ receptor glycosylation and gene expression. *Shock* 42:52–59.
38. Head SA, et al. (2015) Antifungal drug itraconazole targets VDAC1 to modulate the AMPK/mTOR signaling axis in endothelial cells. *Proc Natl Acad Sci USA* 112: E7276–E7285.
39. Strating JR, et al. (2015) Itraconazole inhibits enterovirus replication by targeting the oxysterol-binding protein. *Cell Reports* 10:600–615.